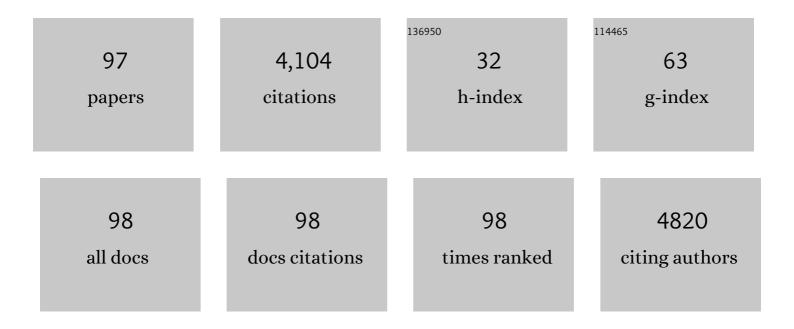
List of Publications by Year in descending order

Source: https://exaly.com/author-pdf/7323299/publications.pdf Version: 2024-02-01



#	Article	IF	CITATIONS
1	Surface-Enhanced Raman Spectroscopy in Single Living Cells Using Gold Nanoparticles. Applied Spectroscopy, 2002, 56, 150-154.	2.2	559
2	XRD analysis of carbon stacking structure in coal during heat treatment. Fuel, 2004, 83, 2427-2433.	6.4	350
3	A sustainable synthesis of nitrogen-doped carbon aerogels. Green Chemistry, 2011, 13, 2428.	9.0	185
4	Adsorptive hydrogen storage in carbon and porous materials. Materials Science and Engineering B: Solid-State Materials for Advanced Technology, 2004, 108, 143-147.	3.5	154
5	Ordered Carbohydrate-Derived Porous Carbons. Chemistry of Materials, 2011, 23, 4882-4885.	6.7	136
6	Investigation of grain boundaries in BaSi2 epitaxial films on Si(1 1 1) substrates using transmission electron microscopy and electron-beam-induced current technique. Journal of Crystal Growth, 2012, 348, 75-79.	1.5	133
7	Structural changes in carbon aerogels with high temperature treatment. Carbon, 2002, 40, 575-581.	10.3	123
8	Structure and solvents effects on the optical properties of sugar-derived carbon nanodots. Scientific Reports, 2018, 8, 6559.	3.3	121
9	Synthesis and Characterization of Copper-Doped Carbon Aerogels. Langmuir, 2002, 18, 7073-7076.	3.5	119
10	Amorphous diamond from C60fullerene. Applied Physics Letters, 1994, 64, 1797-1799.	3.3	104
11	XRD evaluation of KOH activation process and influence of coal rank. Fuel, 2002, 81, 1717-1722.	6.4	94
12	XPS Study of Copper-Doped Carbon Aerogels. Langmuir, 2002, 18, 10100-10104.	3.5	89
13	High-Electrical-Conductivity Multilayer Graphene Formed by Layer Exchange with Controlled Thickness and Interlayer. Scientific Reports, 2019, 9, 4068.	3.3	89
14	Highly (111)-oriented Ge thin films on insulators formed by Al-induced crystallization. Applied Physics Letters, 2012, 101, 072106.	3.3	88
15	XRD evaluation of CO2 activation process of coal- and coconut shell-based carbons. Fuel, 2000, 79, 1461-1466.	6.4	84
16	The Pore Structure Determination of Carbon Aerogels. Adsorption, 1998, 4, 187-195.	3.0	77
17	Preparation and pore control of highly mesoporous carbon from defluorinated PTFE. Carbon, 2003, 41, 1759-1764.	10.3	77
18	70 °C synthesis of high-Sn content (25%) GeSn on insulator by Sn-induced crystallization of amorphous Ge. Applied Physics Letters, 2015, 106, .	3.3	64

#	Article	IF	CITATIONS
19	Synthesis and Characteristics of Graphene Oxide-Derived Carbon Nanosheetâ^'Pd Nanosized Particle Composites. Langmuir, 2010, 26, 6681-6688.	3.5	62
20	The modification of pore size in activated carbon fibers by chemical vapor deposition and its effects on molecular sieve selectivity. Carbon, 1998, 36, 377-382.	10.3	61
21	Molecular beam epitaxy of BaSi2 thin films on Si(001) substrates. Journal of Crystal Growth, 2012, 345, 16-21.	1.5	61
22	MgO-templated nitrogen-containing carbons derived from different organic compounds for capacitor electrodes. Journal of Power Sources, 2010, 195, 667-673.	7.8	59
23	TEM and electron tomography studies of carbon nanospheres for lithium secondary batteries. Carbon, 2006, 44, 2558-2564.	10.3	56
24	Structure and electrochemical properties of carbon aerogels polymerized in the presence of Cu2+. Journal of Non-Crystalline Solids, 2003, 330, 99-105.	3.1	50
25	Nano- and Submicrometer-Sized Spherical Particle Fabrication Using a Submicroscopic Droplet Formed Using Selective Laser Heating. Journal of Physical Chemistry C, 2016, 120, 2439-2446.	3.1	46
26	Title is missing!. Journal of Materials Science, 1998, 33, 199-206.	3.7	44
27	Orientation Control of Large-Grained Si Films on Insulators by Thickness-Modulated Al-Induced Crystallization. Crystal Growth and Design, 2013, 13, 1767-1770.	3.0	44
28	Coal-Based Activated Carbons Prepared with Organometallics and Their Mesoporous Structure. Energy & Fuels, 1997, 11, 327-330.	5.1	43
29	Selective formation of large-grained, (100)- or (111)-oriented Si on glass by Al-induced layer exchange. Journal of Applied Physics, 2014, 115, .	2.5	40
30	Hole Opening of Carbon Nanotubes and Their Capacitor Performance. Energy & Fuels, 2010, 24, 3373-3377.	5.1	39
31	Enhanced Hydrogen Adsorptivity of Single-Wall Carbon Nanotube Bundles by One-Step C <sub>60</sub> -Pillaring Method. Nano Letters, 2009, 9, 3694-3698.	9.1	35
32	Highly enhanced capacitance of MgO-templated mesoporous carbons in low temperature ionic liquids. Journal of Power Sources, 2014, 271, 377-381.	7.8	35
33	Formation of polycrystalline BaSi2 films by radio-frequency magnetron sputtering for thin-film solar cell applications. Thin Solid Films, 2013, 534, 116-119.	1.8	32
34	Preparation of Porous Carbon by Defluorination of Poly(tetrafluoroethylene) and the Effect of Î <sup>3</sup> -Irradiation on the Polymer. Chemistry of Materials, 2001, 13, 2933-2939.	6.7	31
35	Improved Surface Quality of the Metal-Induced Crystallized Ge Seed Layer and Its Influence on Subsequent Epitaxy. Crystal Growth and Design, 2015, 15, 1535-1539.	3.0	30
36	Mesoporous carbon from poly(tetrafluoroethylene) defluorinated by sodium metal. Carbon, 2002, 40, 457-459.	10.3	29

#	Article	IF	CITATIONS
37	Dependence of microscopic structure and swelling property of DTF chars upon heat-treatment temperature. Fuel, 2006, 85, 2064-2070.	6.4	29
38	Lithium-ion intercalation and deintercalation behaviors of graphitized carbon nanospheres. Journal of Materials Chemistry A, 2018, 6, 1128-1137.	10.3	28
39	Direct synthesis of multilayer graphene on an insulator by Ni-induced layer exchange growth of amorphous carbon. Applied Physics Letters, 2017, 110, .	3.3	26
40	High-quality multilayer graphene on an insulator formed by diffusion controlled Ni-induced layer exchange. Applied Physics Letters, 2017, 111, .	3.3	26
41	Lamellar carbon nanosheets function as templates for two-dimensional deposition of tubular titanate. Chemical Communications, 2008, , 4348.	4.1	24
42	Contribution of mesopores in MgO-templated mesoporous carbons to capacitance in non-aqueous electrolytes. Journal of Power Sources, 2015, 276, 176-180.	7.8	23
43	Correlation between the pore structure and electrode density of MgO-templated carbons for electric double layer capacitor applications. Journal of Power Sources, 2016, 305, 128-133.	7.8	23
44	Metal Catalysts for Layer-Exchange Growth of Multilayer Graphene. ACS Applied Materials & Interfaces, 2018, 10, 41664-41669.	8.0	23
45	Fabrication and characterization of mesoporous carbon nanosheets-1D TiO2 nanostructures. Journal of Materials Chemistry, 2010, 20, 2424.	6.7	21
46	Evaluation of accessible and inaccessible microporosities of microporous carbons. Journal of the Chemical Society, Faraday Transactions, 1996, 92, 2297.	1.7	20
47	Title is missing!. Journal of Materials Science, 2001, 36, 4249-4257.	3.7	20
48	Direct synthesis of highly textured Ge on flexible polyimide films by metal-induced crystallization. Applied Physics Letters, 2014, 104, .	3.3	20
49	Molecular Beam Epitaxy of BaSi\$_{2}\$ Films with Grain Size over 4 \$mu\$m on Si(111). Japanese Journal of Applied Physics, 2012, 51, 098003.	1.5	18
50	Double-Layered Ge Thin Films on Insulators Formed by an Al-Induced Layer-Exchange Process. Crystal Growth and Design, 2013, 13, 3908-3912.	3.0	17
51	Large-Grained Polycrystalline (111) Ge Films on Insulators by Thickness-Controlled Al-Induced Crystallization. ECS Journal of Solid State Science and Technology, 2013, 2, Q195-Q199.	1.8	17
52	Orientation control of Ge thin films by underlayer-selected Al-induced crystallization. CrystEngComm, 2014, 16, 2578.	2.6	17
53	TEM observation of heterogeneous polyhedronization behavior in graphitized carbon nanospheres. Materials Science and Engineering B: Solid-State Materials for Advanced Technology, 2008, 148, 245-248.	3.5	16
54	Development and degradation of graphitic microtexture in carbon nanospheres under a morphologically restrained condition. Materials Chemistry and Physics, 2010, 121, 419-424.	4.0	16

#	Article	IF	CITATIONS
55	Silver-induced layer exchange for polycrystalline germanium on a flexible plastic substrate. Journal of Applied Physics, 2017, 122, .	2.5	16
56	Three-step growth of highly photoresponsive BaSi2 light absorbing layers with uniform Ba to Si atomic ratios. Journal of Applied Physics, 2019, 126, .	2.5	16
57	Epitaxy of Orthorhombic BaSi\$_{2}\$ with Preferential In-Plane Crystal Orientation on Si(001): Effects of Vicinal Substrate and Annealing Temperature. Japanese Journal of Applied Physics, 2012, 51, 095501.	1.5	15
58	Orientation control of intermediate-composition SiGe on insulator by low-temperature Al-induced crystallization. Scripta Materialia, 2016, 122, 86-88.	5.2	14
59	Sandwichâ€Type Nanocomposite of Reduced Graphene Oxide and Periodic Mesoporous Silica with Vertically Aligned Mesochannels of Tunable Pore Depth and Size. Advanced Functional Materials, 2017, 27, 1704066.	14.9	14
60	Excellent Rate Capability of MgO-Templated Mesoporous Carbon as an Na-Ion Energy Storage Material. ECS Electrochemistry Letters, 2014, 4, A22-A23.	1.9	13
61	Structure of amorphous hydrogenated carbon film prepared from rf plasma deposition. Carbon, 1993, 31, 1049-1055.	10.3	12
62	Acceleration of graphitization on carbon nanofibers prepared from bacteria cellulose dispersed in ethanol. Carbon, 2012, 50, 4757-4760.	10.3	12
63	Debundling of SWCNTs through a simple intercalation technique. Electrochemistry Communications, 2009, 11, 1441-1444.	4.7	11
64	Quiescent hydrothermal synthesis of reduced graphene oxide–periodic mesoporous silica sandwich nanocomposites with perpendicular mesochannel alignments. Adsorption, 2014, 20, 267-274.	3.0	11
65	Preparation and Characterization of Porous Carbons By Defluorination of Ptfe with Alkali Metals - Effect of Alkali Metals on the Porous Structure Molecular Crystals and Liquid Crystals, 2002, 388, 45-50.	0.9	10
66	Self-organization of Ge(111)/Al/glass structures through layer exchange in metal-induced crystallization. CrystEngComm, 2014, 16, 9590-9595.	2.6	10
67	Multilayer Graphene Battery Anodes on Plastic Sheets for Flexible Electronics. ACS Applied Energy Materials, 2020, 3, 8410-8414.	5.1	10
68	Effects of flexible substrate thickness on Al-induced crystallization of amorphous Ge thin films. Thin Solid Films, 2015, 583, 221-225.	1.8	9
69	Property of upgraded solid product from low rank coal by thermal reaction with solvent. Fuel Processing Technology, 2007, 88, 333-341.	7.2	8
70	Novel Graphitised Carbonaceous Materials for Use as a Highly Corrosionâ€Tolerant Catalyst Support in Polymer Electrolyte Fuel Cells. Fuel Cells, 2010, 10, 960-965.	2.4	8
71	A carbonaceous two-dimensional lattice with FeN <sub>4</sub> units. Chemical Communications, 2018, 54, 8995-8998.	4.1	8
72	Transition process to diamond from C60 fullerene. Chemical Physics Letters, 1994, 226, 595-599.	2.6	7

#	Article	IF	CITATIONS
73	Flow behavior of graphitized carbon black suspensions. Carbon, 2001, 39, 2384-2386.	10.3	7
74	Transfer-free synthesis of highly ordered Ge nanowire arrays on glass substrates. Applied Physics Letters, 2015, 107, 133102.	3.3	6
75	Electrochemical behavior of MgO-templated mesoporous carbons in the propylene carbonate solution of sodium hexafluorophosphate. Journal of Applied Electrochemistry, 2015, 45, 273-280.	2.9	6
76	Microtexture of High Surface Area Activated Carbons. Tanso, 1992, 1992, 295-300.	0.1	6
77	Formation of large-grain-sized BaSi2 epitaxial layers grown on Si(111) by molecular beam epitaxy. Journal of Crystal Growth, 2013, 378, 193-197.	1.5	5
78	Synergetic photocatalysts derived from porous organo Ti–O clusters pillared graphene oxide frameworks (GOFs). RSC Advances, 2014, 4, 60729-60732.	3.6	5
79	Enhanced Durability of Porous Carbon/Single-Walled Carbon Nanotube Composite Electrodes for Supercapacitors. Journal of the Electrochemical Society, 2016, 163, A1753-A1758.	2.9	5
80	Enhancement of the thermoelectric power factor by tuning the carrier concentration in Cu-rich and Ge-poor colusites Cu26+xNb2Ge6â^xS32. Journal of Materials Chemistry C, 2020, 8, 6442-6449.	5.5	5
81	Graphitization behavior of carbon nanofibers derived from bacteria cellulose. Tanso, 2012, 2012, 202, 225-230.	0.1	4
82	Large photoresponsivity in semiconducting BaSi2 epitaxial films grown on Si(001) substrates by molecular beam epitaxy. Journal of Crystal Growth, 2013, 378, 198-200.	1.5	4
83	Electrochemical Behavior of Graphitized Carbon Nanospheres in a Propylene Carbonate-Based Electrolyte Solution. Journal of the Electrochemical Society, 2018, 165, A2247-A2254.	2.9	4
84	TEM and Electron Tomography Imaging of Pt Particles Dispersed on Carbon Nanospheres. Journal of Nano Research, 2010, 11, 119-124.	0.8	3
85	Tem Observation of Metal-Loaded Carbon Aerogels Prepared by an Ion-Exchange Method. Molecular Crystals and Liquid Crystals, 2002, 388, 75-80.	0.9	2
86	Systematic changes in pore size distribution of template carbon obtained via chemical reaction between different cellulose precursors and halogens. Carbon, 2014, 77, 1191-1194.	10.3	2
87	Epitaxy of Orthorhombic BaSi2with Preferential In-Plane Crystal Orientation on Si(001): Effects of Vicinal Substrate and Annealing Temperature. Japanese Journal of Applied Physics, 2012, 51, 095501.	1.5	2
88	Molecular Beam Epitaxy of BaSi2Films with Grain Size over 4 Âμm on Si(111). Japanese Journal of Applied Physics, 2012, 51, 098003.	1.5	2
89	The Structures of Copper-Doped Carbon Aerogels Prepared by an Ion Exchange Method. Materials Research Society Symposia Proceedings, 2001, 697, 8281.	0.1	1
90	Formation of graphite-derived layered mesoporous carbon materials. Microporous and Mesoporous Materials, 2006, 93, 254-262.	4.4	1

#	Article	IF	CITATIONS
91	Epitaxial growth of BaSi2films with large grains using vicinal Si(111) substrates. Physica Status Solidi C: Current Topics in Solid State Physics, 2013, 10, 1756-1758.	0.8	1
92	Fabrication of SrGe2 thin films on Ge (100), (110), and (111) substrates. Nanoscale Research Letters, 2018, 13, 22.	5.7	1
93	Structure and texture of phenol-based carbon nanofibers heat-treated at high temperatures. Tanso, 2013, 2013, 110-115.	0.1	1
94	Effect of Ge/Al thickness on Al-induced crystallization of amorphous Ge layers on glass substrates. Physica Status Solidi C: Current Topics in Solid State Physics, 2013, 10, 1781-1784.	0.8	0
95	Graphene Nanocomposites: Sandwichâ€Type Nanocomposite of Reduced Graphene Oxide and Periodic Mesoporous Silica with Vertically Aligned Mesochannels of Tunable Pore Depth and Size (Adv. Funct.) Tj ETQq1 1	. 017489431	4 rgBT /Over
96	Mechanism of Soot Oxidation over CeO2–ZrO2 under O2 Flow. Bulletin of the Chemical Society of Japan, 2018, 91, 437-443.	3.2	0
97	Structure of porous carbon materials for energy storage applications. Ganseki Kobutsu Kagaku, 2004, 33. 114-120.	0.1	0